# Design and Analysis of Molecular Motifs for Specific Recognition of RNA

Ke Li, M. Fernandez–Saiz,[a] C. Ted Rigl,[a] Arvind Kumar,[a] Kaliappa G. Ragunathan,[b]
Adrian W. McConnaughie,[a] David W. Boykin,[a] Hans-Jörg Schneider[b]
and W. David Wilson*,[a]

[a]*Department of Chemistry, Georgia State University, Atlanta, GA 30303, U.S.A.*
[b]*FR Organische Chemie, Universität des Saarlandes, D-66041 Saarbrüchen, Germany*

**Abstract**—Selective targeting of RNA has become a recent priority in drug design strategies due to the emergence of retroviruses, the need for new antibiotics to counter drug resistance, and our increased awareness of the essential role RNA and RNA structures play in the progression of disease. Most organic compounds known to specifically target RNA are complex, naturally occurring antibiotics that are difficult to synthesize or derivatize and modification of these compounds to optimize interactions with structurally unique RNAs is difficult. The de novo design of synthetically accessible analogues is one possible alternative; however, little is known about the RNA recognition principles on which to design new compounds and limited information on RNA structure in general is available. To contribute to the growing body of knowledge on RNA recognition principles, we have prepared two series of polycationic RNA-binding agents, one with a linear scaffold, the other with a macrocyclic scaffold. We evaluated these compounds for their ability to bind to DNA and RNA, as well as to a specific RNA, the regulatory sequence, RRE, derived from HIV-1, by using thermal melting, circular dichroism, and electrophoresis gel shift methods. Our results suggest that cationic charge centers of high $pK_a$ that are displayed along a scaffold of limited flexibility bind preferentially to RNA, most likely within the major groove. Related derivatives that bind more strongly to DNA more closely mimic classical DNA minor-groove binding agents. Several of the macrocyclic polycations expand on a new binding motif where purine bases in duplex RNA are complexed within the macrocyclic cavity, enhancing base-pair opening processes and ultimately destabilizing the RNA duplex. The results in this report should prove a helpful addition to the growing information on molecular motifs that specifically bind to RNA. © 1997 Elsevier Science Ltd.

## Introduction

Streptomycin (Fig. 1), which binds to RNA, and the actinomycins, which bind to DNA, were among the first compounds identified as promising antibiotics in drug-screening programs that began in the 1930s.[1] The actinomycins generally proved too toxic to be used as antibiotics, but actinomycin D (Fig. 1) was found to have anticancer activity and is still in use in combination chemotherapy.[2] Actinomycin D interacts with DNA through an intercalating phenoxazine ring system with two peptide substituents in the DNA minor groove.[1] Both NMR and X-ray structures have been determined for the actinomycin–DNA complexes, and considerable information is available on the DNA recognition principles for interactions of this type.[3] Streptomycin was the first drug found to be active against *Mycobacterium tuberculosis*. It targets cellular ribosomes, particularly the ribosomal RNA, but there is surprisingly little known about the structure of the complex or the RNA recognition principles used in its formation.[1,4] A number of RNA-binding aminoglycosides (Fig. 1) were discovered shortly after streptomycin, but we also know very little about their interactions with RNA.[1,4] Our poor understanding of drug–RNA interactions is partly due to the complexity of RNA structures and limited information on these structures. Natural RNAs are single-stranded polymers that fold into hairpin duplexes

to give a high percentage of base pairing. These duplexes contain internal loops, base bulges, base-pair mismatches and other noncanonical base interactions that make their structures more complicated and provide sites for highly specific molecular recognition.[5]

We have a significant amount of high-resolution information on complexes of compounds that bind to both DNA and RNA by intercalation, and on compounds that bind in the DNA minor groove.[6,7] Good models also exist for proteins and peptides that bind in the major groove of DNA and RNA.[8,9] There is, however, much less information about antibiotics that bind strongly in the major groove of either DNA or RNA. Structures have been determined for a β-strand peptide from the BIV Tat protein bound to its TAR RNA recognition sequence, as well as for a model of an α-helical peptide from the Rev protein bound in the major groove of the RRE RNA sequence of HIV-1.[10] Both the Tat and Rev peptides contain a high percentage of basic amino acids in their RNA recognition units, and these positively charged side chains make specific contacts within the major groove of RNA, thus confirming the major groove as a good binding site for cationic molecules.[10] The aminoglycosides are incapable of binding to RNA by intercalation and must recognize a groove of RNA structures. The deep major groove of helical RNA with its favorable electrostatic
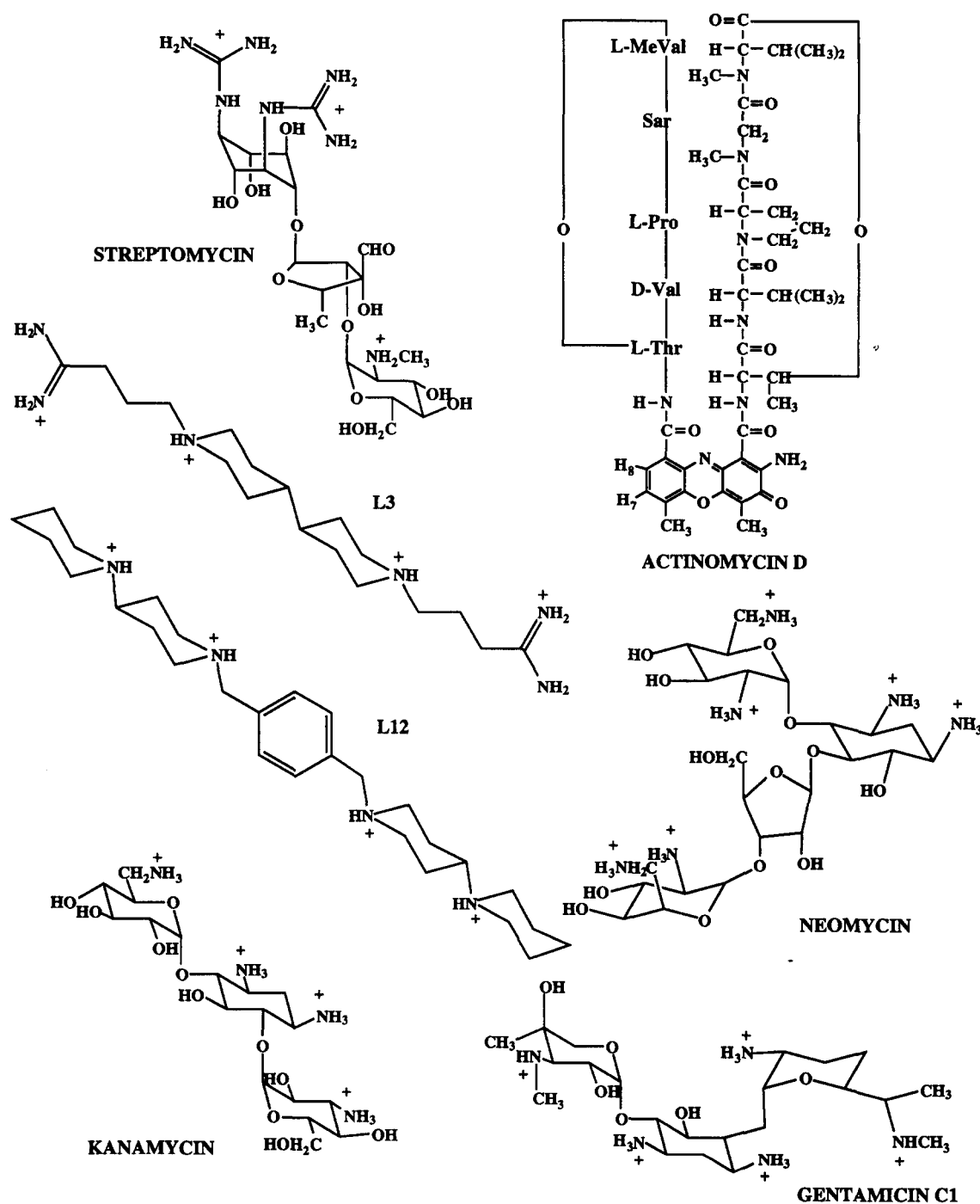
**Figure 1.** Structures of aminoglycosides, actinomycin D, and RNA-binding polycations, arranged to show differences and similarities in structure.

potential for binding cations would appear to be a logical binding site for polycations such as aminoglycosides.[5b] In fact, neomycin B has shown inhibition of the HIV-1 Rev binding to RRE,[11] suggesting that polycationic aminoglycosides interact with the major groove of RNA to block the Rev complex.

The first step in our scheme to design new compounds that target specific RNA structures is to develop lead compounds that can bind strongly to RNA duplexes but have little interaction with related structures such as

isosequential DNA duplexes. Further structural modification of such RNA-specific compounds can lead to the recognition of specific RNA structures. Therefore, our first goal is to design sets of small molecules that will allow us to develop a better understanding of the fundamental complex structures and interactions in RNA duplexes. Such information can then be used to rationally design more selective RNA-binding agents. Compounds with the ability to target specific RNA structures such as RRE and TAR of HIV-1 would obviously have potential for development as antiviral

agents. Given the successful targeting of RNA by polycationic aminoglycoside antibiotics,[11] and the importance of the guanidinium group of arginine in specific peptide–RNA interaction,[12] we have prepared and analyzed the RNA interactions of a variety of structurally relatively simple polycationic compounds (Tables 2, 3, 5, and 6) in order to define the molecular features that provide the most specific RNA binding in such compounds.[13] The aminoglycosides have a relatively rigid framework to display an array of positively charged groups, and the compounds in Tables 2, 3, 5, and 6 were designed to provide simpler, more synthetically accessible molecular scaffolds while maintaining the limited flexibility of the charge array. The structures of two compounds, L3 and L12, from Tables 2 and 3 are shown in Figure 1 for comparison with the structures of several common aminoglycosides. L3 and L12 have four basic groups that are connected by units of variable length and flexibility.

In addition to compounds with linear scaffolds for cationic groups (Tables 2 and 3), macrocyclic (Tables 5 and 6) scaffolds have been designed to arrange the cationic groups.[14] Some of the macrocycles have a cavity that is large enough to allow insertion of bases that are not paired with a complementary base or that will give up pairing on complexation. Compounds of this type offer the additional possibility of recognition of base-bulges and other similar conformational features of complex RNA structures, and they extend the recognition principles for compounds that target RNA duplexes. Earlier studies of linear and macrocyclic polycations indicated that selective RNA binding can be achieved by modulating the overall molecular structure and the position of cationic groups.[13,14] In this paper we describe additional series of linear and macrocyclic polycations and their interaction with RNA and DNA. In addition, specific interactions with HIV-1 RRE RNA evaluated by gel shift are reported. Molecular modeling studies have been used to assist in understanding the molecular mechanisms of the observed RNA–small molecule interactions.

## Results and Discussion

### Aminoglycosides

**1. Thermal melting studies: binding affinity.** The A-form RNA duplex polyA·polyU and the corresponding sequence DNA poly(dA)·poly(dT) have been used, as in previous studies, to provide the initial screen to characterize the interactions of polycationic groove-binding compounds with nucleic acid duplexes. Thermal melting $(T_m)$ studies have been used to compare the binding affinities since these polycations do not have significant spectroscopic signals. At low ratios of compound to nucleic acid bases, biphasic melting curves, which are characteristic of melting of free and bound regions of the nucleic acid, are observed. However, as the ratio is increased the curves become monophasic and approach a limiting value of $\Delta T_m$. The

$\Delta T_m$ values reported in the tables were generally determined at a ratio of 0.3 mol of compound per nucleic acid base and are in the plateau region of the $\Delta T_m$ versus ratio curve. Under these conditions, $\Delta T_m$ values are directly related to equilibrium constants. For some polycation complexes precipitation occurred at the higher ratios and $\Delta T_m$ values are reported at lower ratios. The $T_m$ experiments were done in 0.01 M 2-(N-morpholino)ethanesulfonic acid (MES) buffer at pH 6.2 so that the compounds in Tables 2, 3, 5, and 6 would approach their fully charged state.[15]

The $\Delta T_m$ values for several aminoglycosides were determined for reference (Table 1). Neomycin has five to six charges at pH 6.2[15b] and gave the largest $\Delta T_m$ values with RNA. Gentamicin has close to five charges at pH 6.2 and binds to RNA more strongly than kanamycin, a tetracation, which binds to the RNA more strongly than streptomycin, a trication. None of these compounds gives significant $T_m$ increases with DNA under these conditions. The dication spectinomycin does not show significant binding to either of the nucleic acids duplexes under the conditions of the experiment.

**2. Inhibition of HIV-1 RRE RNA complex formation.** The aminoglycosides were compared for their ability to inhibit the interaction of an RRE duplex model system with a peptide from the HIV-1 Rev protein. We used a specific RNA duplex (Fig. 2) that has been shown to represent the Rev binding element within the larger Rev responsive element (RRE) of HIV-1.[16] An RRE RNA hairpin of similar sequence was shown by Tan et al. to bind with specificity and high affinity to a truncated peptide model of the Rev protein (Rev$_{34-50}$, Fig. 2),[17] which binds in the major groove.[18] In companion studies, the RRE RNA duplex–Rev$_{34-50}$ peptide system demonstrated similar specificity and high affinity and this system has been used to evaluate competitive inhibitors of RRE/Rev interaction.[19] Figure 3 shows that neomycin B is a potent inhibitor of RRE/Rev interaction in this assay and this result is consistent with previous reports.[11,20] Gentamicin inhibits to a slightly lesser degree and streptomycin fails to inhibit the RRE–Rev interaction, again consistent with previous reports.[11] $K_{rel}$ values in this assay were 1.5, 1.4 and not detectable, respectively. Note that neomycin forms

**Table 1.** $\Delta T_m$ values of some nucleic acid-binding antibiotics

| Compd | Basic functions | $\Delta T_m{}^a$ ( °C) | |
|---|---|---|---|
| | | PolyA·polyU | Poly(dA)·poly(dT) |
| Neomycin | 6 | 33.4[b] | ppt[c] |
| Gentamicin | 5 | 22.0 | 1.0 |
| Kanamycin | 4 | 14.3 | 0.5 |
| Streptomycin | 3 | 6.9 | 0.3 |
| Spectinomycin | 2 | 0.0 | 0.0 |

$^a\Delta T_m = T_m$ of the nucleic acid in the presence of drug $- T_m$ of the free nucleic acid in MES buffer with 0.1 M NaCl, pH 6.2 at ratio 0.3.
$^b$Measured at drug:nucleic acid phosphate ratio of 0.1.
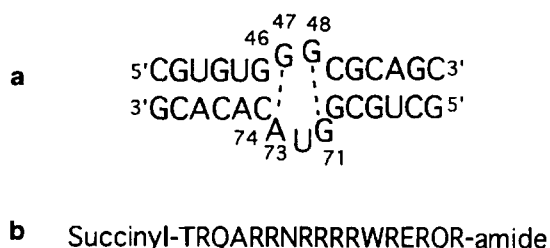$^c$Precipitate formed upon addition of drug.

**a**

$$5'\text{CGUGUG}\overset{46}{\underset{}{\text{G}}}\overset{47}{\underset{}{\text{G}}}\overset{48}{\underset{}{\text{CGCAGC}}}3'$$

$$3'\text{GCACAC}\underset{74}{\underset{}{\text{A}}}\underset{73}{\underset{}{\text{U}}}\underset{71}{\underset{}{\text{G}}}\text{GCGUCG}5'$$

**b**   Succinyl-TRQARRNRRRRWRERQR-amide

**Figure 2.** (a) HIV-1 RRE RNA duplex defined in Pritchard et al.[16c] Noncanonical base interactions are represented by dotted lines.[15b] (b) HIV-1 Rev-related peptide defined in Tan et al.[17]

a specific complex with the RRE RNA duplex that is slightly shifted in this gel assay.

These $T_m$ and inhibition results demonstrate the pronounced affinity aminoglycosides have for RNA duplexes as opposed to DNA. The correlation of $\Delta T_m$ with charge suggests that electrostatic interactions play a dominant role in the RNA interactions; however, DNA and RNA have very similar charge densities and the weak DNA binding demonstrates that more specific interactions are involved in the RNA complex. It seems likely that the aminoglycosides are able to fit into the A-form structure of RNA, probably into the major groove, and form concerted electrostatic interactions that make RNA binding much more favorable than DNA binding.

## Compounds with a bipiperidine central linker

**1. Thermal melting studies.** A series of 1,1'-disubstituted 4,4'-bipiperidine polycations (Table 2), in which imidazoline or amidine functions are attached to the central bipiperidine unit by alkyl (compounds L1–L4) or benzyl (compounds L5–L8) linkers, have been designed as nucleic acid groove-binding agents and their binding affinities evaluated by thermal melting measurements. The central bipiperidine core provides a relatively rigid dicationic unit to which a variety of groups of varying flexibility and physical characteristics can be attached. As shown in Table 2, these compounds form complexes with both RNA and DNA duplexes with $\Delta T_m$ values ranging from 2 to 24 °C for RNA and 8 to >26 °C for DNA. As with the aminoglycosides $\Delta T_m$ determinations were done in the presence of 0.1 M NaCl to minimize nonspecific electrostatic interactions,
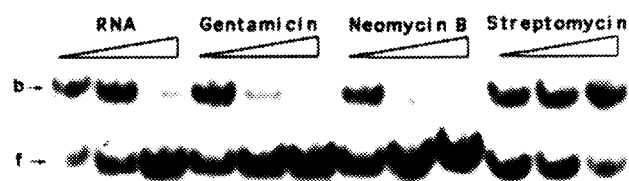
**Figure 3.** Gel shift assay for the inhibitory effect of three aminoglycosides on the formation of the complex between ^{32}P-labeled RRE RNA duplex and Rev[34-50] peptide. Unlabeled (cold) RRE RNA duplex served as a control inhibitor. The positions of bound (b) and free (f) ^{32}P-labeled RRE RNA duplex are indicated.

and at pH 6.2 to approach the fully charged state of the compounds. The results indicate, as with the aminoglycosides, that electrostatic effects contribute significantly to the interactions of these compounds with both RNA and DNA. For example, the hexacations L4 and L8, which have an additional alkylamine substituent on each amidine group, have higher RNA and DNA $\Delta T_m$ values than alkyl-linked (L1–L3) and benzyl-linked (L5–L7) tetracationic compounds, respectively. On the other hand, compound L1, which has the lowest charge due to the proximity of the imidazoline and piperidine groups, has lower $\Delta T_m$ values than compounds L2 and L3 for both RNA and DNA.

Comparison of $\Delta T_m$ values of the tetracations shows significant variations in their RNA and DNA binding and demonstrates that in addition to electrostatic effects, the structural features of these compounds strongly influence their nucleic acid interactions. In both alkyl- and benzyl-linked tetracations, the amidine derivatives L3 and L6 have the highest RNA binding activity in their groups with $\Delta T_m$ values of 17.6 and 10.6 °C, respectively. Alkyl substitution on the amidine group results in decreased RNA binding but has less effect on DNA binding. Compound L7 has an isopropyl group substituted on the amidine group of L6 and has a

**Table 2.** Structure and nucleic acid $\Delta T_m$ values of 4,4'-bipiperidine derivatives

$$\text{R-N}\underset{}{\bigcirc}\underset{}{\bigcirc}\text{N-R}$$

| Compd | R | $\Delta T_m{}^a$ (°C) | |
|-------|---|--------------------|---|
| | | PolyA·polyU | Poly(dA)·poly(dT) |
| L1 | | 7.3 | 5.9 |
| L2 | | 13.3 | 13.6 |
| L3 | | 17.6 | 14.1 |
| L4 | | 24.0[b] | 14.9[b] |
| L5 | | 4.1 | 22.6 |
| L6 | | 10.6 | 22.6 |
| L7 | | 2.2 | 18.0 |
| L8 | | 16.8 | >26.4[b] |

[a] $\Delta T_m = T_m$ of the nucleic acid in the presence of drug $- T_m$ of the free nucleic acid in MES buffer with 0.1 M NaCl, pH 6.2.
[b] Measured at a drug:nucleic acid phosphate ratio of 0.1.

$\Delta T_m$ of only 2.2 °C (a decrease of 8.4 °C compared to **L6**), while maintaining a DNA $\Delta T_m$ of 18 °C (4.6 °C lower than that of **L6**). The RNA $\Delta T_m$ values for the imidazoline compounds **L2** and **L5** are 9 °C and 6.5 °C lower than those of the corresponding amidine compounds **L3** and **L6**, respectively. On the other hand, the DNA $\Delta T_m$ of **L2** is only 0.5 °C lower than **L3** and compound **L5** has the same DNA $\Delta T_m$ as **L6**. The amidine moiety is similar to the guanidinium basic side chain of arginine that is known to interact favorably with the major groove of RNA,[12] and it is clear from the results in Table 2 that amidines also have very favorable RNA interactions.

The RNA $\Delta T_m$ values of the propyl-linked compounds **L2–L4** are 4.5–7.2 °C higher than the corresponding benzyl-linked compounds **L5**, **L6**, and **L8**, whereas their DNA $\Delta T_m$ values are 8.5–11.7 °C lower than those of **L5**, **L6**, and **L8**, indicating that the propyl-amidine/imidazoline moiety favors RNA binding while the benzyl-amidine/imidazoline moiety favors DNA binding. The flexible propyl chain of **L2–L4** probably enhances RNA interactions relative to **L5–L8** by allowing optimal distance and orientation of the charged groups to give more favorable electrostatic interactions with the RNA duplex. The phenyl-amidine/imidazoline units of **L5** and **L6** are similar to those seen in some DNA minor groove-binding agents such as pentamidine, furamidine, and DAPI, and the favorable binding of **L5** and **L6** to DNA (both with $\Delta T_m$ values of 22.6 °C) is consistent with strong interactions with the DNA minor groove at AT sequences.[7] The alkyl-linked compounds apparently do not fit the narrow minor groove of DNA as well as the phenyl linker, thus resulting in significant decreases in DNA $\Delta T_m$ values. This concept is supported by modeling results presented below.

**2. Circular dichroism (CD) analysis.** The binding interaction of polycations **L1–L8** were further studied by CD spectroscopy. On titration of RNA with the polycations in Table 2, CD spectra of the RNA duplex did not show significant changes (data not shown), suggesting that no significant conformational changes in RNA occur on formation of the complexes.

**3. Other tetracations with two piperidinyl groups and general comparisons.** Table 3 lists RNA and DNA $\Delta T_m$ values from previous work[13] for a series of tetracations that also contain two piperidinyl groups, but have the piperidinyl groups separated by a xylenyl or an alkyl linker. Both the xylenyl and the alkyl sets of compounds give similar preferential stabilization of RNA with better RNA interactions for a terminal imidazoline group than for a terminal piperidine. Substitution at the *para-* or *meta-* position of the aromatic ring (**L12** or **L13**) makes little difference in the $\Delta T_m$ values. Chart 1 compares a set of compounds from Tables 2 and 3 that have similar molecular components, but that show a progression in relative affinity for DNA and RNA. Compounds at the top of Chart 1 have the greatest RNA stabilization and the minimum DNA $\Delta T_m$ (for

these tetracations), and the RNA values continually decrease to a minimum at the bottom of the chart while the DNA values continually increase to a maximum $\Delta T_m$. Compounds **L5** and **L11**, for example, each have two piperidine and imidazoline groups and either one or two phenyl rings. Strong stabilization of DNA and weak RNA interactions are observed with **L5** while with **L11** the opposite results are obtained. Compounds **L2** and **L9** also contain two piperidine and imidazoline groups, but have either one or two propyl chains. With **L2** moderate stabilization of both DNA and RNA is obtained while with **L9** significantly less DNA stabilization is observed, but the RNA $\Delta T_m$ increases significantly. Chart 1 illustrates quite clearly that compounds with similar molecular components and the same charge can be designed to interact quite differently with RNA and DNA. As with aminoglycosides, these

**Table 3.** Structure and nucleic acid $\Delta T_m$ values of some polycations[13]

| Compd | Structure | $\Delta T_m{}^a$ ( °C) PolyA·polyU | $\Delta T_m{}^a$ ( °C) Poly(dA)·poly(dT) |
|---|---|---|---|
| **L9** |  | 18.1 | 6.1 |
| **L10** |  | 9.8 | 3.3 |
| **L11** |  | 16.2 | 8.7 |
| **L12** |  | 8.1 | 3.5 |
| **L13** |  | 8.0 | 3.3 |

$^a\Delta T_m = T_m$ of the nucleic acid in the presence of drug $- T_m$ of the free nucleic acid in MES buffer with 0.1 M NaCl, pH 6.2.



| | RNA $\Delta$Tm | DNA $\Delta$Tm | RNA $\Delta$Tm / DNA $\Delta$Tm |
|---|---|---|---|
| **L9** | 18.1 | 6.1 | 2.97 |
| **L11** | 16.2 | 8.7 | 1.86 |
| **L2** | 13.3 | 13.6 | 0.98 |
| **L5** | 4.1 | 22.6 | 0.18 |

**Chart 1.** Comparison of structure and relative RNA and DNA binding activity of some linear scaffold tetracations.

linear cations show that both structure and charge are important for their nucleic acid interactions. The linear cations, however, are much less efficient than aminoglycosides in distinguishing the A-form RNA helix from the B-form structure of DNA.

## 4. Inhibition of HIV-1 RRE RNA complex formation.

Since the compounds in this paper were designed to be synthetically accessible mimetics of aminoglycoside antibiotics we determined the ability of several linear polycations to inhibit the formation of RRE–Rev complex using competitive gel shift assays for comparison with the aminoglycoside results (Fig. 3). Two assay formats were utilized as described in the Experimental: (1) selected compounds were added at concentrations as high as 100 μM to solutions containing labeled, free RRE RNA duplex and the reaction mixtures were assayed by gel shift to determine if the compounds formed a complex with RRE RNA duplex that is stable to partition during gel electrophoresis (results not shown);[21] and (2) compounds were added to solutions containing RRE RNA duplex and Rev$_{34-50}$ peptide, and were assayed to determine the relative inhibitory effect ($K_{rel}$) each compound has against the formation of the RRE–Rev complex (Fig. 4).

Neomycin B clearly forms a complex with the RRE RNA duplex that is stable to partition during gel electrophoresis. The complex is significantly less mobile than the labeled, free RRE RNA duplex band. The $K_{rel}$ value of 1.54 demonstrates that neomycin is a remarkable inhibitor of the RRE/Rev interaction in this system, as in the RRE hairpin–Rev protein assay used by Zapp et al.[11]

Compounds L1, L2, and L6 have the lowest $\Delta T_m$ values for polyA·polyU (Table 2) and they neither formed a complex with the RRE RNA duplex that was stable to gel partition nor inhibited RRE/Rev interaction.
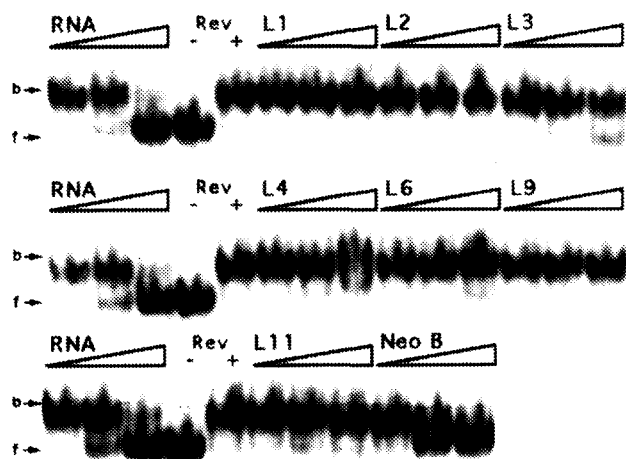


**Figure 4.** Gel shift assay for RRE/Rev inhibition by a series of linear polycations. Figure symbols are analogous to Figure 3. The reaction mixtures in lane 4 (Rev −) contain no Rev$_{34-50}$ peptide. Lane 5 (Rev +) contains Rev$_{34-50}$ peptide, as do all other lanes.

Compounds L3, L9, and L11 had significantly higher $\Delta T_m$ values for polyA·polyU (Tables 2 and 3), yet no gel-stable complexes with the RRE RNA duplex could be detected. However, compound L3 did reproducibly demonstrate slight inhibition of the RRE/Rev interaction (Fig. 4). Interestingly, the $\Delta T_m$ value of compound L3 is similar to the $\Delta T_m$ values of L9 (Tables 2 and 3). These $\Delta T_m$ values are determined in pH 6.2 MES buffer, while the buffer used in the gel shift assay has a pH of 7.6. Therefore, thermal denaturation of the RRE RNA duplex with L3 and L9 at pH 7.0 was analyzed in order to examine pH effects. The results (Table 4) show that at pH 7.0, only L3 binds significantly to the RRE RNA duplex ($\Delta T_m$ 4.3 °C at saturation), but no significant increase for L9 was obtained. Similar decreases in $\Delta T_m$ with polyA·polyU at pH 7 were observed for L9 and L11 but not L3 complexes (data not shown). This indicates that the RNA-binding activity of L9 and L11 is more sensitive to pH change than that of L3, and this may be responsible for the lack of inhibitory activity of L9 and L11 against the RRE–Rev complex at pH 7.6. Although L9 and L11 have their piperidinyl groups separated by either a propyl or phenyl spacer, the p$K_a$ value of the piperidinyl nitrogen, which is approximately 10 as an isolated function, is markedly reduced by its proximity to the imidazoline group. L3, on the other hand, has greater separation between the two piperidinyl nitrogens, as well as equivalent or greater separation between these groups and the imidazoline functions. This finding suggests that spacing of three methylene units between charge centers can be insufficient in some contexts and this should be considered in the development of RNA recognition principles and drug design strategies.

Compound L4, with six basic functions, binds to polyA·polyU with the highest affinity, as assessed by thermal denaturation studies at 0.1 molecules per base pair (Table 2), and L4 forms a complex with the RRE RNA duplex that is shifted in gel partition experiments. The shifted L4/RRE RNA duplex species interferes with the determination of $K_{rel}$ in Figure 4. Further studies showed that L4 does not significantly inhibit the RRE/Rev interaction (results not shown). Clearly, RNA-binding by organic cations in Tables 2 and 3, as determined by thermal denaturation studies, is correlated with inhibition of RRE/Rev interaction, however, these compounds are much weaker inhibitors of the Rev–RRE complex than neomycin (Fig. 4). The fact that compound L3 inhibits RRE/Rev interaction suggests that it binds in the major groove of RRE, as does Rev,[10] in agreement with the modeling studies described below.

## 5. Molecular modeling.

To help understand the differences in RNA interactions observed for the four compounds in Chart 1, each was docked with a 12 base-pair RNA model, A$_{12}$·U$_{12}$, for polyA·polyU and energy minimized as described in the Experimental. Initial comparisons of the docked and minimized complexes of the compounds with both the major and minor grooves of the model RNA duplex revealed much better

**Table 4.** $\Delta T_m$ values ( °C) for linear polycations, **L3** and **L9**, with RRE RNA duplex at pH 6.2 and 7.0[a]

| pH: | 6.2 | 7.0 | | | | | | |
|---|---|---|---|---|---|---|---|---|
| Ratio:[b] | 30 | 2 | 4 | 7 | 10 | 15 | 20 | 30 |
| **L3** | 4.9 | −0.7 | 0.6 | 1.0 | 1.7 | 2.7 | 3.6 | 4.3 |
| **L9** | 4.9 | −0.5 | 0.7 | 0.0 | −0.3 | −0.3 | 0.7 | 1.0 |

[a]The $T_m$ for the RRE RNA duplex (2 μM) at pH 6.2 is 55.2 °C. The $T_m$ at pH 7.0 is 53.5 °C.
[b]Ratios are compound per duplex.

energetics in the major-groove complex as expected from the design of the compounds. To evaluate the major-groove interactions in more detail, constraints were applied to bring the charged groups of the compounds close to the phosphate charges at the edge of the major groove of the RNA A-form helix. Good electrostatic contacts between protonated amines and the phosphate oxygen atoms were maintained when the complex was re-minimized with the removal of the distance constraints. The minimized complexes of each compound with the RNA duplex reveal that in all cases a low-energy structure with a narrowed major groove is formed. There are a number of structural differences in each model which appear to explain the differences in binding affinities obtained from the biophysical results. The general structure of the complexes is illustrated by a minimized model of **L9** complexed with the 12-mer RNA (Fig. 5). The other complexes are not illustrated but are discussed below.

Compound **L9** was found to match the interphosphate distances very well and the minimized complex gave good electrostatic contacts with phosphate oxygen atoms (1.9–2.3 Å). The rotational flexibility of the imidazoline–piperidine function allows each cationic group to obtain favorable contacts to a nearby phosphate. The distance between the charged imidazoline and the quaternary nitrogen of piperidine closely matches those of the anionic phosphate backbone in RNA, thereby allowing concerted recognition of the phosphate backbone. The small, flexible propyl linker also allows rotational freedom in the ligand structure and the linker is able to lie close to the backbone of the helix without unfavorable steric clash.

Compound **L5** contains the central 4,4-bipiperidine linking group and the aryl-imidazoline unit commonly used in DNA minor groove-binding compounds.[7] As before, good contacts are obtained in the model, but the results highlight a number of problems with the complex and suggest a reason why such structural analogues of DNA minor-groove binders do not bind well to duplex RNA. First, although the imidazoline N–H atoms can span the interphosphate distance readily, the imidazoline and the phenyl ring adopt a co-planar arrangement that forces the hydrophobic aromatic ring to lie in close proximity to the phosphate backbone with interatomic distances between aryl-hydrogen and anio-

nic oxygen atoms of $\approx 2.5$ Å. The overall greater rigidity of this ligand compared to **L9** prevents facile co-operative matching of the protonated imidazoline sites to the anionic backbone without the introduction of an energetically unfavorable interaction of the phenyl group with the phosphate backbone. The central
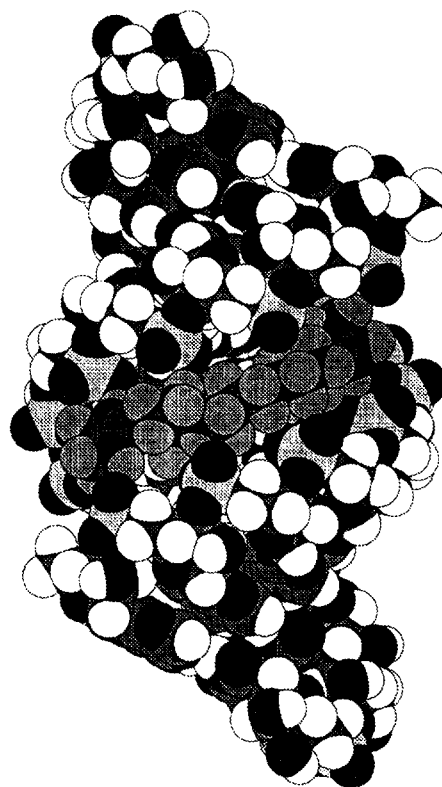


**Figure 5.** A space-filling model of **L9** docked into the major groove of $A_{12} \cdot U_{12}$ and energy minimized as described in the Methods section. The shading increases for hydrogens (white), phosphorous (light gray), to carbon, nitrogen, and oxygen is the darkest gray. **L9** is in the center of this view and its hydrogens are shaded gray to help in its visualization. One imidazoline can be seen at the lower left and the other at the upper right. As can be seen easily at the lower left, the two NH groups of the imidazolines hydrogen-bond to phosphates on opposite sides of the RNA major groove. From the lower left to the upper right, the first piperidinyl NH points down and interacts with a phosphate oxygen. The propyl linker is in the center of the drawing and the upper piperidinyl NH points up to interact with a phosphate oxygen on the upper strand. Clearly an advantage of this compound for binding to RNA lies in its appropriate spacing of charges for concerted interactions with RNA phosphates.

4,4'-bispiperidine core of **L5** can readily make additional contacts to the phosphate backbone on opposite strands of the duplex RNA via the two tertiary amines, but this group is likely to be more sterically demanding than the simple propyl linker of **L9** and may also contribute to the poor overall RNA binding observed for this compound. Compound **L2** differs from **L5** by replacing the phenyl ring adjacent to the imidazoline function with a propyl group. The substantial increase in RNA binding for **L2** relative to **L5** is consistent with the above modeling results in that the phenyl/imidazoline moiety of **L5** is unfavorable for effective RNA binding. Removal of the phenyl group restores rotational freedom to the imidazoline group and removes the energetically unfavorable interactions of the backbone with the phenyl ring.

Replacement of the central propyl chain of **L9** with a xylenyl moiety (compound **L11**) results in only a slight decrease in RNA-binding affinity. Modeling of RNA complexes of this compound predicts good contacts between protonated ligand sites and the anionic backbone with interatomic distances of approximately 2 Å. A comparison with results for compound **L5** shows that moving the phenyl group away from the imidazoline to a central position, **L11**, results in substantial restoration of RNA binding. Furthermore, the result highlights the 4-imidazolylpiperidine group as an effective unit for RNA binding. The central phenyl group of **L11** is located in an unfavorable hydrophilic site at the groove entrance, as with **L5**, but this does not seem to affect the overall binding to polyA·polyU RNA to a large extent. We therefore conclude that the strong binding affinity for **L9** is due primarily to the 4-imidazolylpiperidine moiety which appears to dominate its binding to duplex RNA.

In the minimized complexes, the standard width of the RNA major groove decreases by approximately 3 Å to enable close contacts between the ligand and the phosphate oxygens. Such a narrowing is not uncommon in RNA structures since a number of X-ray crystal structures of tRNAs reveal a substantial variation in major groove width over a relatively short base-pair length.[5] The modeling results suggest that the groo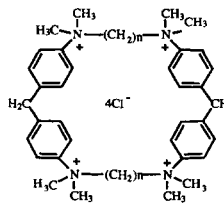ve width is deformable to allow optimization of complex structures. A major-groove binding mode is suggested for polycations arrayed along a linear scaffold and the modeling results provide explanations for the $\Delta T_m$ differences observed in Chart 1. The polycationic macrocycles discussed below offer additional motifs that could assist in the design of RNA-binding agents.

## Macrocyclic cations

**1. Thermal melting studies.** Macrocyclic systems provide very attractive scaffolds for specific charge and hydrogen-bonding interactions with RNA. We have previously shown that the cationic cyclophanes in Table 5 can stabilize RNA when the cyclophane cavity is small ($n = 3$), but can actually destabilize RNA duplexes when the cavity is large enough to allow insertion of a purine base ($n = 6$) into the cyclophane cavity.[14] At low ratios of compound to RNA only stabilization of RNA, caused primarily by electrostatic interactions of the cations with RNA phosphates, is seen. At higher levels, increased stabilization is observed for CP33, but destabilization, a decreased $T_m$ relative to the free RNA, is observed for CP66.[14] Interestingly, for DNA of corresponding sequence only stabilizing effects are seen for all cyclophanes at all ratios (Table 5). These results with CP33-66 provide a model for interpreting results for other macrocyclic complexes with RNA and DNA and for design of additional macrocycles for specific recognition of RNA. The macrocycles in Table 6 are related to those in Table 5 in charge and functional groups, but the two sets of compounds differ significantly in structure.[14] The methylene-linked phenyl rings of the CP compounds (Table 5) provide the organizing structure for the cyclophane cavity while in **C1–C7** (Table 6) either a biphenyl or a phenyl-type group determines the cavity shape and preorganization of the macrocycle.

The $\Delta T_m$ values for RNA and DNA complexes, as in Tables 1–3, are given for RNA complexes in Table 6 as a function of compound to DNA ratio for **C1–C7**, and representative $T_m$ curves are shown in Figure 6. Many of the compounds caused precipitation, or had broad $T_m$ curves at the highest ratios, indicating some aggregation under these conditions. The $\Delta T_m$ results are given at

**Table 5.** Structure and nucleic acid $\Delta T_m$ values of CPnn compounds

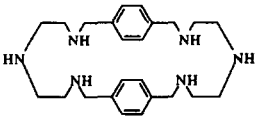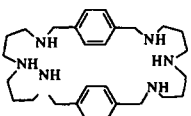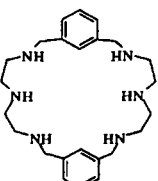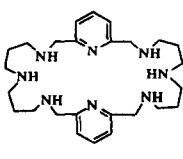| Compd | | | $\Delta T_m$[a] (°C) | | NaCl added |
|---|---|---|---|---|---|
| | | | Poly(da)·poly(dT) | PolyA·polyU | |
| CP33 | $n = 3$ | | 29.8 | 27.2 | None |
| | | | 3.9 | 10.6 | 0.05 M |
| CP44 | $n = 4$ | | 35.9 | 14.1 | None |
| | | | 4.2 | 2.6 | 0.05 M |
| CP55 | $n = 5$ | | 28.6 | 6.3 | None |
| | | | 3.6 | −2.0 | 0.05 M |
| CP66 | $n = 6$ | | 27.4 | −5.8 | None |
| | | | 3.6 | −5.5 | 0.05 M |
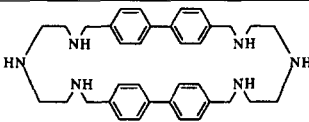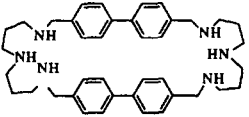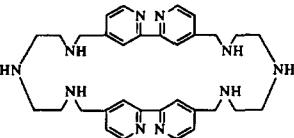
[a]The experiments were conducted in MES buffer without any additon of salt and with 0.05 M NaCl, at a ratio of 0.2 mol of CPnn per mol of nucleic acid phosphate. $\Delta T_m = T_m$ complex $- T_m$ nucleic acid.

low salt concentration and either at 0.05 NaCl (for weaker binding compounds) or at 0.1 M NaCl. Note that $\Delta T_m$ values in Tables 1–3 are at 0.1 M NaCl, indicating stronger RNA binding for the aminoglycosides and linear cations than for the macrocycles at this salt concentration.

Modeling studies by Schneider and co-workers indicate that all of the compounds containing only two phenyl groups have cavities that are too small to bind a purine base,[14] and all of those compounds (C4–C7) cause much

larger increases in the $T_m$ values for RNA than for DNA. The $\Delta T_m$ values are a function of salt concentration (Table 6), but large $T_m$ increases for RNA are caused by C5 and C7 up to 0.1 M NaCl concentration. The RNA $T_m$ curves for C5 in Figure 6 are biphasic at the 0.05 ratio (compound:base) with a low melting phase characteristic of free RNA and a high melting phase for the complex. At a 0.1 ratio the high melting phase is dominant. As can be seen, this compound as well as C7 (Table 6) has very large $\Delta T_m$ increases even at the higher salt concentration. At higher ratios both

**Table 6.** Structure and nucleic acid $\Delta T_m$ of macrocyclic cations[a]

| Compd | $\Delta T_m$ (polydA·polydT) | | | $\Delta T_m$ (polyA·polyU) | | | NaCl added |
|---|---|---|---|---|---|---|---|
| | $r = 0.1$ | $r = 0.2$ | $r = 0.3$ | $r = 0.1$ | $r = 0.2$ | $r = 0.3$ | |
| C1 | –<br>5.4 | 23.9<br>9.1 | 24.4<br>8.6 | 5.0<br>–7.1/–0.7 | 3.7<br>–7.1/10 | –5.4<br>broad | none<br>0.05 M |
| C2 | –<br>4.1 | 18.8<br>4.7 | 19.1<br>broad | 14.1<br>4.1 | 13.7<br>0.8 | ppd<br>ppd | none<br>0.05 M |
| C3 | 13.5<br>0.9 | 18.1<br>2.3 | 20.3<br>3.6 | 13.2<br>0.4 | ppd<br>0.8 | ppd<br>–2.6 | none<br>0.05 M |
| C4 | 3.7/16.3<br>broad<br>2.7 | 23.3<br><br>6.2 | 23.8<br><br>6.8 | 34.9<br>14.9<br>broad | 38.6<br>19.0 | 49.6<br>20.8 | none<br>0.05 M |
| C5 | above 40<br>biphasic | 19.3 | broad | 53.9<br>34.9 | ppd<br>broad | ppd<br>ppd | none<br>0.1 M |
| C6 | 4.7<br>2.2 | 14.3<br>3.6 | broad<br>5.9 | 34<br>123.1 | 37.2<br>13.4 | 41.2<br>23.7 | none<br>0.05 M |
| C7 | above 40<br>biphasic | 18.2 | broad | 54<br>27 | 56.7<br>27/37.1 | ppd<br>ppd | none<br>0.1 M |

[a]The experiments were conducted in MES buffer, 0.001 M EDTA and pH 6.25, [Na$^+$] = 0.007 M and with addition of 0.005 M NaCl, at ratios 0.1, 0.2, and 0.3 mol of compound per mol of nucleic acid phosphate.
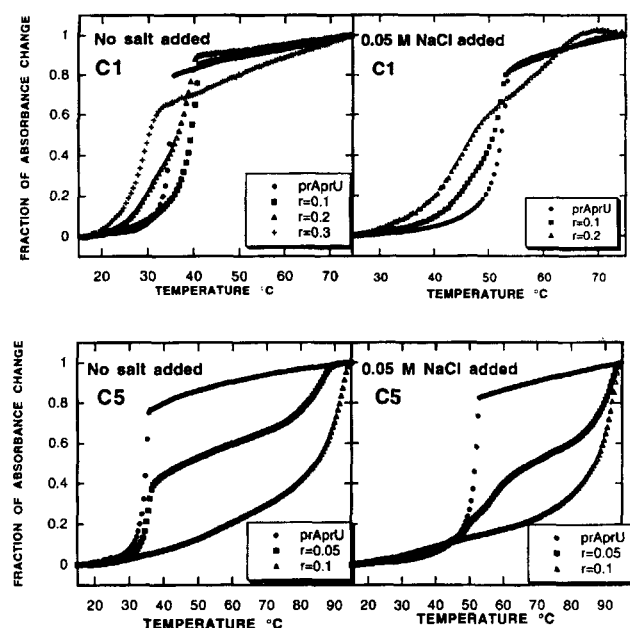
**Figure 6.** $T_m$ curves in MES buffer without any addition of salt, and with 0.05 M NaCl for polyA·polyU (l) with C1 at ratios 0.1 (■), 0.2 (△), and 0.3 (+); and for C5 at ratios 0.05 (■) and 0.1 (△) mol of compound per mol of nucleic acid phosphate.

**Table 7.** Inhibition of formation of complex between RRE and Rev as assessed by gel shift assay

| Compound | $K_{rel}$[a] |
|---|---|
| Neomycin B | 1.54 |
| CP33 | nd |
| CP33 | nd |
| CP44 | nd |
| CP55 | 0.01 |
| CP66 | nd |
| C1 | nd |
| C2 | nd |
| C3 | nd |
| C4 | nd |
| C5 | 0.06 |
| C6 | nd |
| C7 | 0.02 |

[a]$K_{rel}$ is the reciprocal of the concentration of competitor required to reduce by 50% Rev binding to $^{32}$P-labeled RRE RNA duplex divided by the reciprocal concentration required of the unlabeled (cold) RRE RNA duplex (control) to achieve the same level of inhibition (variation of Pritchard et al.[16]). This rendering means that strong competitive inhibitors have $K_{rel}$ values greater than 1.0. The notation, nd, means that inhibition was not detected.

C5 and C7 cause RNA precipitation. The difference between *meta*- and *para*-substitution on the phenyl ring in this series has little effect on their $\Delta T_m$ values (compare C4 with C6). A two methylene linker between amine functions causes a significant p$K_a$ decrease relative to three or more methylene units,[14b] and compounds with the two methylene linker cause smaller $T_m$ increases than related derivatives with a three methylene linker (compare C4 with C5). The compounds C4–C7 have much larger $\Delta T_m$ values than any of the cyclophanes from Table 6 or the biphenyl-type compounds (C1–C3) in Table 6. It is clear that they can fit into one of the RNA grooves, probably the major groove for the reasons described above, and dramatically stabilize RNA duplexes. As expected for these polycations, they cause larger $T_m$ increases at low salt than with 0.05 M added NaCl (Table 6).

The biphenyl compound C1 is large enough to allow insertion of a purine base into the macrocycle cavity,[14b] and the $T_m$ curves for C1 shown in Figure 6 are quite different from those for C5. As with CP66 (Table 5), C1 causes an increase in RNA $T_m$ at low ratios, but decreases the RNA $T_m$ as the ratio is increased. The curves have complex shapes, as expected for their complex RNA interactions, but the decrease in RNA melting temperature is easily seen. All three of the biphenyl-type macrocycles (C1–C3) cause small increases in RNA $T_m$ at a ratio of 0.1 and low salt concentration. Compound C2 causes a similar increase at 0.2 and precipitates at the 0.3 ratio. Precipitation at ratios above 0.2 is also observed at higher NaCl concentrations. C3 gives a $T_m$ increase at the 0.1 ratio, but no $T_m$ value can be obtained at higher ratios and low

salt concentration. At a salt concentration of 0.05 M NaCl, only small $T_m$ increases are obtained with C3–RNA complexes at ratios of 0.1 and 0.2, and at a ratio of 0.3 a slight decrease is observed.

**2. CD studies.** CD spectra of the RNA complexes help to explain the differences in melting results for the mono- and biphenyl derivatives (Fig. 7). The CD spectra of RNA in the presence of macrocyclic compounds fall into three groups that are represented by spectra of RNA complexes with C1, C5, and CP66 in Figure 7. With the CP compounds (Table 5) no significant CD changes were obtained for RNA complexes with the compounds that cause $T_m$ increases, CP33–CP55.[14] With CP66, however, large decreases in RNA CD signals were observed as the amount of compound was increased (Fig. 7), and the RNA spectrum approached that of denatured RNA at ratios of approximately 0.3 with no added salt. None of the compounds caused a significant change in the DNA CD spectrum up to a ratio of 0.3. As shown in Table 5, the CP66 RNA interactions are quite salt concentration dependent, and the CD changes are much smaller at 0.05 M NaCl than at lower salt (Fig. 7).

The C1–C7 macrocycles in Table 6 also cause quite different changes in the RNA CD spectrum depending on whether they have the phenyl or biphenyl-type units. With the phenyl compounds (C4–C7), represented by C5 in Figure 7, the CD signal at 265 nm increases while the band for 220–230 nm decreases and shifts to longer wavelengths. This result indicates that the strong interaction with and stabilization of RNA by C4–C7 causes a slight rearrangement of the duplex. With C1 (Fig. 7), the CD signals decrease as with CP66 and the CD spectrum approaches that for denatured RNA as the ratio increases. The hyperchromicity of the C1 $T_m$ curves decreases markedly as the ratio is increased, and
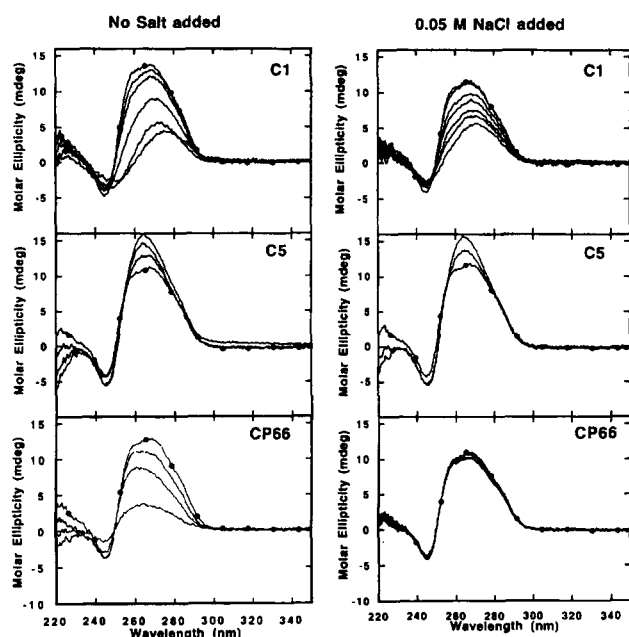
**Figure 7.** CD spectra obtained in MES buffer at 20 °C with addition of 0.05 M NaCl and without any salt added, for the titration of polyA-polyU (l) with **C1**, **C5**, and **CP66**. The titration was carried out by increasing the ratio of compound per mol of nucleic acid phosphate by 0.1 for each successive addition. **C5** showed signs of aggregation above a ratio of 0.3 in the no salt condition and also above a ratio of 0.2 when 0.05 M NaCl was added. The free RNA CD spectrum is shown with black circles.



**Figure 8.** Gel shift assay for RRE/Rev inhibition by a series of cyclic polycations. Figure symbols are analogous to Figure 4. $K_{rel}$ values are shown in Table 7.

the CD results indicate that this is due to progressive unfolding of the duplex as the concentration is increased. CD results with **C2** (not shown) at low salt are somewhat different. The CD initially changes very little as the ratio is increased to 0.2, but decreases significantly at 0.3, indicative of the onset of unfolding. At 0.05 M added salt only small CD changes are obtained for **C2** complexes. The results with **C3** (not shown) are very much like those obtained with **C1** at low salt concentrations and indicate a progressive opening of the RNA duplex with the increase of the concentration. At 0.05 M salt the CD changes with **C3** are much less than with **C1**, as also observed with CP66 (Fig. 7).

As a control, both CP66 and **C1** were added to the RNA dinucleotide, r(ApA), which has no base-pair interactions. No change in CD is obtained on addition of CP66 or **C1** to this RNA strand at ratios up to 0.3 (spectra not shown). This indicates that the CD changes described for CP66 and **C1** with the RNA polymer are primarily due to interaction with extruded polymer bases followed by opening of the polymer duplex to strands, and not to any induced CD of the macrocycle–RNA complex structure. NMR studies (not shown) indicate that both **C1** and CP66 bind to the dimer, but that any nucleotide conformation is retained in the complex, and the interaction does not affect the dimer CD spectrum. This observation is supported by calculations with CP66 and a trinucleotide by Schneider and co-workers (unpublished), showing that after energy minimization
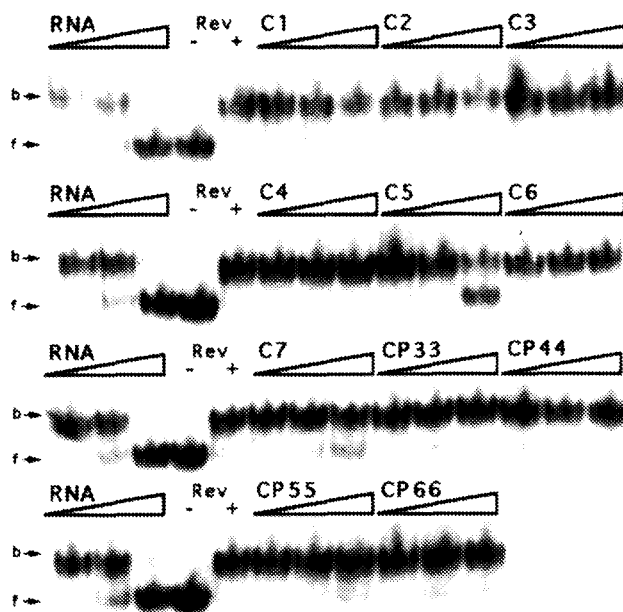
there are no significant conformational changes in the small single-stranded trimer.

The $T_m$ and CD results present a consistent view of the interaction of **C1–C7** with RNA and DNA. All of the compounds bind to DNA and stabilize the complex. The stabilization drops off significantly as the salt concentration is increased, however, **C5** and **C7** maintain strong interactions even at 0.1 M NaCl (Table 6). The compounds with two phenyl rings all stabilize RNA with the most dramatic effects obtained for **C5**. Even at 0.10 M salt concentration **C5** causes large increases in the RNA $T_m$ and significant changes in the RNA CD curves. **C1** has a completely different effect on RNA $T_m$ and CD. The RNA melting temperature increases slightly at low ratio and then decreases as more **C1** is added. These results are similar to those observed for CP66 and are characteristic of an initial slight electrostatic stabilization of the duplex followed by base-pair opening and eventual denaturation of the RNA duplex at higher ratio. The CD curves of RNA decrease on increasing the ratio of **C1** and approach that of single-stranded RNA at high ratio. The duplex stabilization appears to be controlled primarily by electric interactions while the base-pair opening reaction is driven by the favorable energetics of insertion of a base into the **C1** cyclophane cavity as observed with CP66.

**3. Interaction with HIV-1 RRE RNA.** The strongest RNA-binding cyclic cations from Tables 5 and 6 were assayed by gel shift as described above for compounds in Tables 1–3. Gel shift studies suggest that **C5** forms a complex with RRE RNA duplex that is stable to partition during gel electrophoresis (data not shown), and **C5** demonstrated clear inhibition of the Rev–RRE

complex (Fig. 8 and Table 7). **C7** showed no stable complex with RRE RNA duplex, but did inhibit RRE/Rev interaction to a significant degree. CP55 also formed no gel stable complexes with the RNA duplex, but did inhibit the Rev–RRE complex to a detectable degree.

Many of the cyclic polycations shown in Tables 5 and 6 bind RNA with high affinity as assessed by thermal denaturation studies of polyA·polyU. The series shows particularly strong binding in 10 mM MES at pH 6.2; however, the electrostatic interactions between the polycations and the phosphate backbone are markedly diminished in the environment at the higher pH and salt concentration used in the gel shift studies.

## Conclusions

Aminoglycosides represent some of our best paradigms for the specific binding of small molecules to RNA, and their structural and chemical features strongly suggested that specific targeting of RNA could be accomplished by displaying an array of cationic centers along a scaffold of limited flexibility. In our effort to develop more synthetically accessible compounds based on this paradigm, two classes of scaffolds were explored in the work described in this paper, a linear combination of cationic heterocycles and a macrocyclic structure bearing cationic functions. We have demonstrated that several compounds within these two classes do indeed target RNA with significant specificity. The molecular motifs held in common by these agents clearly define several RNA recognition principles that will assist in the development of RNA-specific organic molecules. In addition, several compound motifs bind preferentially to DNA and these results could be useful in the further development of DNA-selective minor-groove binding agents.[7,22,23] These results underscore the differences in recognition principles between relatively simple forms of polymeric RNA and DNA duplexes used in this study, and suggest that even greater differences could be exploited in more complex RNA structures to achieve greater specificity. A strong RNA-binding compound is clearly the first step, and more subtle modifications should enable one to address specific RNA structures.

The major groove of RNA is the binding site of important viral regulatory proteins such as Tat and Rev in HIV-1, making the major groove an attractive target for antiviral drug design. The structure of the aminoglycosides suggest that they bind to the major groove of RNA, a conclusion that is supported by the ability of neomycin B to competitively displace Rev protein, as well as Rev-related peptide, from its binding site on RRE RNA. Cationic functionalities are characteristic of these RNA-binding proteins, peptides, and antibiotics, and clearly strong interactions of small molecules with the major groove of RNA will generally require cations.

Table 1 shows that the total number of basic groups and compound charge on aminoglycosides is directly related to binding affinity for RNA. The aminoglycosides strongly stabilize RNA but do not significantly stabilize DNA. This is in contrast with the compounds in Table 2 which bind to both DNA and RNA. An increase in binding affinity for both RNA and DNA was observed when amine functions are added to **L3** and **L7** to achieve **L4** and **L8**. The ratio of RNA $\Delta T_m$:DNA $\Delta T_m$ decreases with this modification, clearly showing that the addition of two cationic amine functions does not emulate, in terms of RNA specificity, the addition of, for example, one of the diaminohexane or pyranose functions common to the aminoglycosides. Charge is clearly part of the story, but structure plays a key role in the discrimination of DNA and RNA by these small cations.

The spatial arrangement of the cationic charge centers affect both the $pK_a$ values of the cationic functions, as well as the contacts formed with anionic phosphate oxygens and other functions within the major groove of RNA. The change in $\Delta T_m$ values with pH illustrates the importance of charge and $pK_a$ on RNA interactions. **L9** produced the highest RNA $\Delta T_m$:DNA $\Delta T_m$ ratio, suggesting that this spatial arrangement might be worth reproducing with charge centers of higher $pK_a$. Propyl spacers are also used in **C5** and the transition to ethyl groups in **C6** is marked by a significant decrease in DNA and RNA affinities. The RNA $\Delta T_m$:DNA $\Delta T_m$ ratio for **C6** is the highest of the compounds under study. However, the compound showed no binding to the RRE RNA duplex under gel shift conditions and this is probably due primarily to the reduced $pK_a$ values for the more closely spaced secondary amine cations.

Molecular motifs that are conducive to RNA but not DNA binding and vice versa are apparent in Tables 2 and 3. The most striking example of these RNA-binding motifs is the aliphatic linker used to attach charge centers as shown in **L3**. Attachment of charges by a rigid, hydrophobic phenyl group as in **L6** both reduces binding of RNA and increases binding of DNA. Stabilization of DNA by the benzyl amidine function in **L6** is consistent with a number of DNA minor-groove binders.[22,23] Note, however, that binding affinity for polyA·polyU has been shown to be only loosely related to binding to specific, structural RNAs. For example, an N-substituted furamidine analogue that features the same benzyl amidine function was shown to bind polyA·polyU with lower affinity than for other related compounds in the series, yet this analogue demonstrated the highest binding affinity in the series for RRE RNA and, in addition, was the most potent inhibitor of RRE/Rev interaction.[24] But as an RNA recognition principle, the hydrophilic environment of the RNA major groove is apparently appropriate for accessible, charged groups, while the more hydrophobic minor groove of DNA prefers planar, aromatic charged motifs.

Modeling studies of the compounds in this report (Tables 1 and 2) suggest that the RNA major groove becomes narrower to provide stronger interactions between phosphate and cationic groups of compounds **L2**, **L5**, **L9**, and **L11** (Chart 1). The aminoglycosides, on the other hand, may be more effective at presenting amine functions to anionic oxygens and cause less structural perturbation of RNA. There is a precedent for larger compounds making favorable contacts in this region since Rev is known to bind in the major groove of RRE.[10,18a]

De novo drug designers and developers of combinatorial libraries are seeking RNA recognition principles that could, for example, rule out functions that are not conducive to RNA binding and rule in functions that not only bind with specificity in the major groove of RNA, but also feature functions that are synthetically accessible and derivatizable. We have described several functions and structural motifs that impart specificity for RNA with lower affinity for DNA. The compounds in this study clearly do not yet approach the exquisite specificity of the aminoglycosides; however, the progress in identifying relatively simple components that have relatively high ratios of binding to RNA and that inhibit the Rev–RRE complex is encouraging. Additional derivatives in this series that incorporate functions of high p$K$ that interact strongly with RNA such as the guanidinium group, should further enhance RNA-binding affinity.

## Experimental

### Materials

HPLC-purified RNA sequences for the RRE RNA duplex model (Fig. 2) were purchased from Midland (Tx). Oligonucleotides used for the RRE RNA duplex were end-labeled using [$\gamma$-$^{32}$P] ATP and T4 polynucleotide kinase under standard conditions (Amersham). A Rev-related peptide with the sequence defined by Tan et al.,[17] succinyl-TRQARRNRRRRWRERQR-amide (Rev$_{34-50}$), was synthesized as described in Rigl et al.[19]

### Thermal melting measurements

Thermal denaturation studies of poly(dA)·poly(dT) and polyA·polyU (Sigma Chemical Co.) were conducted on Varian Cary 3 or Cary 4 spectrometers interfaced to Dell/486 microcomputers as previously described.[13] $T_m$ values in the absence and presence of compounds were determined in 0.01 M MES buffer containing 1 mM EDTA, pH 6.3. Varying concentrations of NaCl were added to the buffer as indicated in the figures and tables. $T_m$ values for RRE RNA duplex in the absence and presence of compounds were determined in MES buffer, as well as in 0.01 M phosphate buffer containing 1 mM EDTA, 0.1 M NaCl, pH 7.0.

### Circular dichroism

CD spectra were obtained with a Jasco J-710 spectrophotometer interfaced to an IBM computer as previously described.[13] All CD experiments were performed at 20 °C in 1-cm path length cuvettes with $4.5 \times 10^{-5}$ M RNA base concentration. Spectra were obtained at several ratios of compound to nucleic acid base in MES buffer with varying concentrations of NaCl and were averages of three to four scans.

### Molecular modeling

The cationic ligands were generated using the Tripos SYBYL 6.0 package on a Silicon Graphics 4D/25 computer. Charges for each compound were assigned and calculated with the MNDO module of SYBYL, and the compounds were minimized to an RMS gradient of 0.01 kcal/mol·Å$^2$ using a distance-dependent dielectric constant of the form $\varepsilon = 4rij$. The RNA sequence (A$_{12}$·U$_{12}$) was built using the A-form helix fiber diffraction data of Arnott and co-workers.[25] The structure was prepared with terminal 5'- and 3'-OH groups and minimized to an RMS gradient of 0.08 kcal/mol · Å$^2$ as previously described.[26]

Ligands were manually docked into either the major groove or the minor groove of the RNA helix, avoiding any unfavorable steric clashes, and positioned approximately centrally in the entrance to the groove. For more detailed analysis of major-groove interactions, appropriate contacts between protonated amines and phosphate oxygens on the backbone were selected, constrained to a distance of 2 Å and minimized to an RMS gradient of 0.08 kcal/mol·Å$^2$. The minimized complexes were then re-minimized with the distance constraints removed to an RMS gradient of 0.08 kcal/mol·Å$^2$ to allow unfavorable contacts to be removed.

### Competitive gel shift assays

The RRE RNA duplex was formed by heating complementary $^{32}$P-labeled strands at micromolar concentrations to 90 °C for 2 min in 10 mM phosphate, 1 mM EDTA, 0.1 M NaCl, pH 7.0 buffer. After cooling to room temperature, the RRE RNA duplex was diluted to 25 nM in a binding reaction buffer. RRE RNA duplex-containing solutions were aliquoted (8 µL) and competitive inhibitors were added (2 µL) to the vials at increasing concentrations. Unlabeled (cold) RRE RNA duplex served as a control inhibitor.[27] Rev$_{34-50}$ was then added (2 µL) to achieve a final peptide concentration of 6 µM. The final reaction conditions were 10 mM phosphate, 1 mM EDTA, 0.1 NaCl, 1 mM MgCl$_2$, 1 mM DTT, 170 µg/mL tRNA (Sigma yeast tRNA, catalog number R-8759) and 10% glycerol. The reaction mixtures were incubated for 15 min in an ice bath and samples (3 µL) were applied to a 12% nondenaturing polyacrylamide gel cast in 1X TBE that had been equilibrated for 2 h.[24] The samples were electrophoresed for 4 h at 220 V at 4–8 °C. The gels were fixed,

## Synthesis

Synthesis of **L9–L13**,[13] CP66,[14] and **C1–C7**[28] are reported elsewhere.

**1,1′-Bis(4-cyanobenzyl)-4,4′-bipiperidine (6a).** A mixture of 4,4′-bispiperidine (5.04 g free base, 0.03 mol), 4-cyanobenzylbromide (11.76 g, 0.06 mol) and anhydrous potassium carbonate (8.28 g, 0.06 mol) in 60–70 mL of absolute ethanol was heated under reflux for 7–8 h (followed by silica gel TLC in $CHCl_3$:MeOH:$NH_3$ 15:4:1), the solvent removed under vacuum and the residue stirred with ice-water. The solid was filtered, washed with water, dried in air, redissolved in 80–100 mL of chloroform and chromatographed over silica gel. Elution with ether, chloroform, and chloroform:methanol:ammonia (15:4:1) afforded the product which was recrystallized from ether:chloroform (3:1) to give 7.5 g (63%) of a white crystalline solid: mp 210–211 °C; IR (KBr) 3060, 2931, 2919, 2900, 2765, 2224, 1606, 1502, 1467, 1363, 1324, 1130, 1064, 986, 821, 783 cm⁻¹; ¹H NMR ($CDCl_3$) δ 7.5 (d, 4H, $J$ = 7.8 Hz), 7.43 (d, 4H, $J$ = 7.8 Hz), 3.5 (s, 4H), 1.98–1.88 (m, 4H), 1.67–1.62 (m, 4H), 1.3–1.06 (m, 6H); ¹³C NMR δ 144.7, 131.8, 129.3, 118.8, 110.6, 62.7, 54.1, 40.6, 29.4; MS $m/e$ 398 (M⁺). Anal. calcd for $C_{26}H_{30}N_4$ (398.53): C 78.37, H 7.58, N 14.06; found: C 78.44, H 7.62, N 13.97.

**1,1′-Bis(4-amidinobenzyl)-4,4′-bipiperidine tetrahydrochloride (L6).** The bisnitrile (2.5 g, 6.3 mmol) was suspended in 40 mL of absolute ethanol, cooled in an ice–salt bath and dry HCl gas was passed until saturation. The stoppered flask was stirred at room temperature for three to four days (monitored by IR for the disappearance of the band for the cyano group), diluted with dry ether to precipitate imidate ester hydrochloride, filtered, washed with dry ether and dried under vacuum at 35 °C for 4–5 h to afford 3.8 g (77%).

Dry ammonia was passed through a cold suspension of imidate ester hydrochloride (0.95 g, 1.5 mmol) in 15 mL of absolute ethanol until saturated and stirred at room temperature for two days. The solvent was removed under vacuum and the resulting solid was dissolved in ice–water, basified to pH >9 with 2 M NaOH, extracted with 3 × 20 mL of chloroform, dried under vacuum and recrystallized from ether:hexane (3:1) to afford 0.5 g (77%) of the free base as a white solid: mp 205 °C dec.

The free base (0.43 g, 1 mmol) was suspended in 5 mL of absolute ethanol, 5 mL of saturated ethanolic HCl was added and the mixture was stirred at 40 °C for 30 min. The volume was reduced to 5 mL by rota-evaporation and the remaining mixture was diluted with dry ether. The resulting white solid was filtered, washed with dry ether and dried under vacuum at 75 °C for 12 h yielding 0.5 g (82%) of the product: mp 270–

273 °C dec; ¹H NMR (DMSO-$d_6$) δ 7.90 (d, 4H, $J$ = 8.0 Hz), 7.83 (d, 4H, $J$ = 8.0 Hz), 4.37 (s, 4H), 3.38–3.33 (m, 4H), 3.00–2.90 (m, 4H), 1.91–1.81 (m, 4H), 1.91–1.81 (m, 4H), 1.62–1.36 (m, 6H); ¹³C NMR (DMSO-$d_6$/$D_2O$) δ 164.8, 133.3, 130.7, 128.1, 127.2, 58.4, 51.4, 35.6, 24.9; MS $m/e$ 432 (M⁺). Anal. calcd for $C_{26}H_{36}N_6$·4HCl·1.5$H_2O$ (605.49): C 78.37, H 7.58, N 14.06; found: C 78.44, H 7.62, N 13.97.

**1,1′-Bis[(4-imidazolinyl)benzyl]-4,4′-bipiperidine tetrahydrochloride (L5).** Freshly distilled ethylenediamine (0.36 g, 6.0 mmol) was added under nitrogen to a suspension of imidate ester hydrochloride (0.95 g, 1.5 mmol) from **6a** in 10 mL of absolute ethanol. The reaction mixture was refluxed for 12 h, excess ethanol distilled under vacuum and the residue diluted with ice–water, stirred and filtered. The aqueous filtrate was basified with 2 M NaOH to pH above 9 and the turbid solution was extracted with 3 × 20 mL of $CHCl_3$, dried over anhydrous $Na_2SO_4$, filtered and concentrated under vacuum. The residue was crystallized from $CHCl_3$:ether (1:4) to afford 0.53 g (73%) of the free base as a white solid: mp 250–252 °C dec.

The free base (0.48 g, 1 mmol) was suspended in 10–15 mL of absolute ethanol, saturated with dry HCl gas and stirred at 40 °C for 30 min. The solvent was distilled in vacuum, the residue was triturated with dry ether and the white solid was filtered, washed with dry ether and dried in vacuum at 75 °C for 24 h to afford 0.52 g (79%) of the product: mp 308–310 °C; ¹H NMR ($D_2O$/DMSO-$d_6$) δ 8.0 (d, 4H, $J$ = 8.4 Hz), 7.84 (d, 4H, $J$ = 8.4 Hz), 4.38 (brs, 4H), 4.04 (s, 8H), 3.80–3.32 (m, 4H), 3.09–2.93 (m, 4H), 1.96–1.80 (m, 4H), 1.60–1.41 (m, 6H); ¹³C NMR (DMSO-$d_6$/$D_2O$) δ 165.6, 136.5, 133.5, 130.1, 124.7, 60.75, 53.9, 45.9, 37.7, 27.3; MS $m/e$ 484 (M⁺). Anal. calcd for $C_{30}H_{40}N_6$·4HCl·1.5$H_2O$ (655.56): C 54.96, H 7.22, N 12.82; found: C 54.88, H 7.41, N 12.80.

**1,1′-[4-(Isopropylamidino)benzyl]-4,4′-bipiperidine tetrahydrochloride (L7).** To the stirred suspension of imidate ester hydrochloride (0.95 g, 1.5 mmol) from **6a** in 15 mL of absolute ethanol was added isopropylamine (0.35 g, 6 mmol). The reaction mixture was stirred at room temperature for 12 h, the solvent removed under vacuum, and the residue dissolved in 10 mL of ice–water, filtered, and basified to pH 10 with 2 M NaOH. The turbid precipitate was extracted with 4 × 25 mL of chloroform, the solvent removed under vacuum, and the product recrystallized from chloroform: ether (4:1) to give 0.51 g (55%) of the product as a white solid: mp 155–157 °C dec; ¹H NMR (DMSO-$d_6$) δ 7.59 (d, 4H, $J$ = 8.0 Hz), 7.25 (d, 4H, $J$ = 8.0 Hz), 6.20 (s, 2H), 3.80 (sep, 2H, $J$ = 6.3 Hz), 3.41 (s, 4H), 2.82–2.75 (m, 4H), 1.91–1.81 (m, 4H), 1.62–1.55 (m, 4H), 1.24–0.96 (m, 6H), 1.10 (d, 12H, $J$ = 6.30 Hz).

The free base (0.41 g, 0.8 mmol) was dissolved in 6–7 mL of absolute ethanol, treated with 6–7 mL of saturated ethanolic HCl and stirred at 60 °C for 2 h. The solvent was removed under vacuum, and the residue was stirred with 30 mL of dry ether and filtered.

dried under vacuum at 80 °C, and autoradiographed (Biomax, Kodak) for up to one week. Autoradiographs were scanned and quantitated (PDI, Inc.).

The resulting white solid was dried under vacuum at 80 °C for 24 h to generate 0.48 g (87%) of the product: mp 285–290 °C dec; $^1$H NMR (DMSO-$d_6$) δ 7.75 (s, 8H), 4.30 (s, 4H), 4.05–4.00 (sep, 2H, $J$ = 6.3 Hz), 3.33 (brs, 2H), 2.9 (m, 4H), 1.87 (brs, 2H), 1.61–1.35 (m, 6H), 1.29 (d, 12H, $J$ = 6.3 Hz); $^{13}$C NMR (DMSO-$d_6$/D$_2$O) δ 161.0, 134.8, 131.4, 129.6, 128.3, 57.8, 51.2, 37.1, 25.2, 20.9; MS $m/e$ 516 (M$^+$). Anal. calcd for C$_{32}$H$_{48}$N$_6$·4HCl·1.5H$_2$O (589.62): C 65.40, H 9.09, N 14.30, found: C 65.13, H 9.22, N 14.19.

### 1,1′-Bis{4-[N(3-dimethylaminopropyl)amidino]-benzyl}-4,4′-bipiperidine hexahydrochloride (L8).

To a suspension of imidate ester hydrochloride (0.95 g, 1.5 mmol) from 6a in 10 mL of absolute ethanol was added dry N,N-dimethyl-1,3-propane diamine (0.61 g, 6 mmol). The reaction mixture was stirred under nitrogen at room temperature for 12 h, and the solvent was removed in vacuum; the residue was dissolved in ice–water and filtered. The filtrate was basified to pH 10–11, extracted with 3 × 25 mL of chloroform, dried over anhydrous Na$_2$SO$_4$ and concentrated under vacuum. The resulting white solid was recrystallized from ether:CHCl$_3$ yielding 0.7 g (78%) of the free base: mp 168–170 °C.

The free base (0.63 g, 1 mmol) in 10 mL of absolute ethanol was saturated with dry HCl gas and stirred at 40 °C for 1 h. The solvent was removed in vacuum, the residue triturated with dry ether and the very hygroscopic white solid was filtered and dried in vacuum at 80 °C for 24 h yielding 0.70 g (82%) of the product: mp 290–292 °C dec; $^1$H NMR (D$_2$O/DMSO-$d_6$) δ 7.96 (d, 4H, $J$ = 8.2 Hz), 7.85 (d, 4H, $J$ = 8.2 Hz), 4.51 (s, 4H), 3.75–3.64 (m, 6H), 3.46–4.40 (m, 4H), 3.06 (s, 12H), 2.38–2.32 (m, 4H), 2.14–2.11 (m, 4H); $^{13}$C NMR (DMSO-$d_6$/D$_2$O) δ 165.6, 135.7, 133.5, 131.5, 130.0, 61.2, 56.4, 44.4, 41.4, 38.4, 27.7, 23.9; FAB MS $m/e$ 603 (M$^+$+1). Anal. calcd for C$_{36}$H$_{58}$N$_8$·6HCl·2H$_2$O (857.67): C 50.41, H 7.99, N 13.06; found: C 50.13, H 8.11, N 12.91.

### 1,1′-Bis(cyanomethyl)-4,4′-bipiperidine (1a).

Reaction of 4,4′-bipiperidine and chloroacetonitrile as described for the synthesis of 6a gave 1a in 71% yield, mp 185–188 °C dec; IR (KBr) 2222 cm$^{-1}$; $^1$H NMR (DMSO-$d_6$) δ 3.72 (s, 4H), 2.79 (brs, 2H), 2.75 (brs, 2H), 2.06 (dt, 4H, $J$ = 2.1 Hz, $J$ = 6.6 Hz), 1.67 (brs, 2H), 1.63 (brs, 2H), 1.50 (dq, 4H, $J$ = 3.3 Hz, $J$= 12.0 Hz), 1.04–0.95 (m, 2H); $^{13}$C NMR (CDCl$_3$) δ 114.7, 52.6, 46.3, 39.4, 28.9; MS $m/e$ 246 (M$^+$). Anal. calcd for C$_{14}$H$_{22}$N$_4$ (246.36): C 68.26, H 9.00, N 22.74; found: C 68.29, H 9.03, N 22.65.

### 1,1′-Bis[(2-imidazolinyl)methyl]-4,4′-bipiperidine tetrahydrochloride (L1).

Reaction of ethylene diamine with the bisimidate ester hydrochloride from 1a as described for the synthesis of L5 gave L1 as a white hygroscopic solid in 71% yield, mp 265–268 °C; $^{13}$C NMR (DMSO-$d_6$/D$_2$O/35 °C) δ 166.9, 58.3, 55.0, 39.9, 37.5, 27.2; MS $m/e$ 332 (M$^+$). Anal. calcd for C$_{18}$H$_{32}$N$_6$·4HCl·1.5H$_2$O

(505.37): C 42.77, H 7.78, N 15.92; found: C 43.00, H 7.61, N 16.01.

### 1,1′-(3-Cyanopropyl)-4,4′-bipiperidine (3a).

Reaction of 4-chlorobutyronitrile and 4,4′-bipiperidine (free base) as described for 6a gave 3a in 68% yield, mp 113–115 °C; IR (KBr) 2242 cm$^{-1}$; $^1$H NMR (CDCl$_3$) δ 2.88 (brs, 8H), 2.85 (brs, 2H), 2.41–3.36 (m, 8H), 1.94–1.77 (m, 8H), 1.68 (brs, 2H), 1.64 (brs, 2H), 1.32–1.11 (m, 4H), 1.08–0.99 (m, 2H); $^{13}$C NMR (CDCl$_3$) δ 116.6, 56.6, 54.1, 40.8, 29.4, 23.0, 14.8; MS $m/e$ 302 (M$^+$). Anal. calcd for C$_{18}$H$_{30}$N$_4$ (302.45): C 71.47, H 9.99, N 18.52; found: C 70.86, H 10.03, N 18.34.

### 1,1′-Bis(3-amidinopropyl)-4,4′-bipiperidine tetrahydrochloride (L3).

The imidate ester hydrochloride from 3a was converted to the amidine free base as described for the synthesis of L6 in 68% yield, mp 160–161 °C.

On treatment with ethanolic HCl, the free base yielded the hydrochloride salt as a white crystalline solid in 86% yield, mp >330 °C dec; $^1$H NMR (DMSO-$d_6$/D$_2$O) δ 3.53 (brs, 2H), 3.49 (brs, 2H), 3.06 (t, 4H, $J$ = 7.8 Hz), 2.89 (t, 4H, $J$ = 12 Hz), 2.50 (t, 4H, $J$ = 7.8 Hz), 2.13–2.02 (m, 4H), 1.90 (brs, 2H), 1.62–1.38 (m, 6H); $^{13}$C NMR (DMSO-$d_6$/D$_2$O) δ 176.5, 57.9, 53.9, 40.6, 33.6, 29.1, 22.5; FABMS $m/e$ 337 (M$^+$+1). Anal. calcd for C$_{18}$H$_{36}$N$_6$·4HCl·H$_2$O (504.90) C 42.81, H 8.48, N 16.64; found: C 43.76, H 8.00, N 16.19.

### 1,1′-[3-(2-Imidazolino)propyl]-4,4′-bipiperidine tetrahydrochloride (L2).

Reaction of ethylenediamine with bis-imidate ester hydrochloride from 3a as described for L5 gave 57% free base of L2 as a white solid: mp 178–180 °C dec, which was converted to its hydrochloride salt in 84% yield, mp 288–289 °C dec; $^1$H NMR (DMSO-$d_6$/D$_2$O) δ 3.57 (brs, 8H Hz), 2.94 (brs, 2H), 2.92 (brs, 2H), 2.83 (t, 4H, $J$ = 6.8 Hz), 2.35 (t, 4H, $J$ = 6.8 Hz), 1.86 (dt, 4H, $J$ = 6.8, $J$ = 1.6 Hz), 1.79 (t, 4H, $J$ = 6.8 Hz), 1.71 (brs, 2H), 1.68 (brs, 2H), 1.29 (dt, 4H, $J$ = 6.8 Hz, $J$ = 1.6 Hz), 1.10–1.03 (m, 2H); $^{13}$C NMR (DMSO-$d_6$/D$_2$O) δ 171.2, 56.6, 54.3, 45.7, 38.3, 27.6, 24.7, 21.3; FABMS $m/e$ 389 (M$^+$+1). Anal. calcd for C$_{22}$H$_{40}$N$_6$·4HCl·H$_2$O (552.46): C 47.82, H 8.39, N 15.21; found: C 47.84, H 8.10, N 15.17.

### 1,1′-Bis{3[N-3-(dimethylaminopropyl)amidino]propyl}-4,4′-bipiperidine hexahydrochloride (L4).

Reaction of 3-dimethylaminopropylamine and bis-imidate ester hydrochloride from 3a as described for L8 yielded free base of L4 (61%) as a hygroscopic gummy mass, which was converted to its hydrochloride salt as a white solid in 80% yield: mp 268–270 °C dec; $^1$H NMR (DMSO-$d_6$/D$_2$O) δ 3.49 (brs, 2H), 3.45 (brs, 2H), 3.26 (t, 4H, $J$ = 6.6 Hz), 3.12–2.97 (m, 8H), 2.90–2.80 (m, 4H), 2.74 (s, 12H), 2.51 (m, 4H), 2.15–1.78 (m, 12H), 1.57–1.30 (m, 6H); $^{13}$C NMR (DMSO-$d_6$/D$_2$O) δ 167.8, 56.5, 56.0, 54.2, 44.1, 40.5, 38.1, 31.0, 27.5, 23.5, 22.4; FABMS $m/e$ 507 (M$^+$+1). Anal. calcd for (770.6): C 43.63, H 9.02, N 14.54; found: C 44.21, H 8.81, N 14.82.

## References

1. Waring, M. J. In *The Molecular Basis of Antibiotic Action*, Gale, E. F.; Cundliffe, E.; Reynolds, P. E.; Richmond, M. H.; Waring, M. J., Eds.; Wiley: London, 1881; p 287, 2nd ed.

2. Frei, E., III. *Cancer Chemother. Rep*. **1974**, *54*, 49.

3. (a) Wilson, W. D.; Li, Y.; Veal, J. In *Advances in DNA Sequence Specific Agents*; Hurley L. H., Ed.; JAI: Greenwich, 1992; Vol. 1, p 89. (b) Scott, E. V.; Jones, R. L.; Banville, D. L.; Zon, G.; Marzilli, L. G.; Wilson, W. D. *Biochemistry* **1988**, *27*, 915. (c) Scott, E. V.; Zon, G.; Marzilli, L. G.; Wilson, W. D. *Biochemistry* **1988**, *27*, 7940. (d) Kamitori, S.; Takusagawa, F. *J. Mol. Biol*. **1992**, *225*, 445. (e) Kamitori, S.; Takusagawa, F. *J. Am. Chem. Soc*. **1994**, *116*, 4154.

4. Cundliffe, E. In *The Ribosome: Structure, Function, and Evolution*; Hill, W. E.; Dahlberg, A.; Garrett, R. A.; Moore, P. B.; Schlessinger, D.; Warner, J. R., Eds.; American Society of Microbiology: Washington, D.C., 1990; p 479.

5. (a) Tinoco, I., Jr. *J. Phys. Chem*. **1996**, *100*, 13311. (b) Lavery, R.; Pullman, B. *Nucleic Acids Res*. **1981**, *9*, 4677.

6. Wilson, W. D. In *Comprehensive Natural Products Chemistry* Vol. 7, DNA and Aspects of Molecular Biology, Kool, E., Ed; Elsevier Science: Oxford, in press.

7. Geierstanger, B. H.; Wemmer, D. E. In *Annual Review of Biophysics and Biomolecular Structure*; Stroud, R. M., Ed.; Annual Reviews: Palo Alto, 1995; p 463.

8. (a) Ellenberger, T. *Curr. Opin. Struct. Biol*. **1994**, *4*, 12. (b) Raumann, B. E.; Brown, B. M.; Sauer, R. T. *Curr. Opin. Struct. Biol*. **1994**, *4*, 36.

9. (a) Nagai, K. *Curr. Opin. Struct. Biol*. **1996**, *6*, 53. (b) Nagai, K.; Mattaj, I. W. *RNA-Protein Interactions*; IRL: Oxford, 1994.

10. (a) Puglisi, J. D.; Chen, L.; Blanchard, S.; Frankel, A. D. *Science* **1995**, *270*, 1200. (b) Ye, X; Kumar, A.; Patel, D. J. *Chem. and Biol*. **1995**, *2*, 827. (c) Leclerc, F.; Cedergren, R.; Ellington, A. D. *Nature Struct. Biol*. **1994**, *1*, 293. (d) Scanlon, M. J.; Fairlie, D. P.; Craik, D. J.; Englebretsen, D. R.; West, M. L. *Biochemistry* **1995**, *34*, 8242. (e) Battiste, J. L.; Mao, H.; Rao, N. S.; Tan, R.; Muhandiram, D. R.; Kay, L. E.; Frankel, A. D.; Williamson, J. R. *Science* **1996**, *273*, 1547.

11. Zapp, M. L.; Stern, S.; Green, M. R. *Cell* **1993**, *74*, 969.

12. (a) Tao, J.; Frankel, A. D. *Biochemistry* **1996**, *35*, 2229; Connell, G. J.; Illangesekare, M.; Yarus, M. *Biochemistry* **1993**, *32*, 5497. (c) Puglisi, J. D.; Tan, R.; Calnan, B. J.; Frankel, A. D.; Williamson, J. R. *Science* **1992**, *257*, 76. (d) Famulok, M. *J. Am. Chem. Sic*. **1994**, *116*, 1698.

13. McConnaughie, A. W.; Spychala, J.; Zhao, M.; Boykin, D.; Wilson, W. D. *J. Med. Chem*. **1994**, *37*, 1063.

14. (a) Fernandez-Saiz, M.; Schneider, H.-J.; Sartorius, J.; Wilson, W. D. *J. Am. Chem. Soc*. **1996**, *118*, 4739. (b) Ragunathan, K. G.; Schneider, H.-J. *J. C. S. Perkins Trans*. **1997**, in press.

15. (a) Perrin, D. D. *Dissociation Constants of Organic Bases in Aqueous Solution*; Butterworths: London, 1965. (b) Botto, R. E.; Coxon, B. *J. Am. Chem. Soc*. **1983**, *105*, 1021.

16. (a) Cullen; B. R.; Malim, M. H. *Trends in Biochem. Sci.* **1991**, *16*, 346. (b) Bartel, D. P.; Zapp, M. L.; Green, M. R.; Szostak, J. W. *Cell* **1991**, *67*, 529. (c) Pritchard, C. E.; Grasby, J. A.; Hamy, F. Zacharek, A. M.; Singh, M.; Karn, J.; Gait, M. J. *Nucleic Acid Res*. **1994**, *22*, 2592.

17. Tan, R.; Chen, L.; Buettner, D. H.; Frankel, A. D. *Cell* **1993**, *73*, 1031.

18. (a) Battiste, J. L.; Tan, R.; Frankel, A. D.; Williamson, J. R. *J. Biomol. NMR* **1995**, *6*, 375. (b) Peterson, R. D.; Bartel, D. P.; Szostak, J. W.; Horvath, S. J.; Feigon, J. *Biochemistry* **1994**, *33*, 5357.

19. Rigl, C. T.; Lloyd, D. H.; Tsou, D. S.; Gryaznov, S. M.; Wilson, W. D. *Biochemistry* **1997**, *36*, 650.

20. (a) Werstuck, G.; Zapp, M. L.; Green, M. R. *Chemistry & Biology* **1996**, *3*, 129. (b) Symensma, T. L.; Giver, L.; Zapp, M.; Takle, G. B.; Ellington, A. D. *J. Virology* **1996**, *70*, 179.

21. Weeks, K. M.; Crothers, D. M. *Biochemistry* **1992**, *31*, 10281.

22. Boykin, D. W.; Kumar, A.; Spychala, J.; Zhou, M.; Lombardy, R. J.; Wilson, W. D.; Dykstra, C. C.; Jones, S. K.; Hall, J. E.; Tidwell, R. R.; Laughton, C.; Nunn, C. M.; Neidle, S. D. *J. Med. Chem*. **1995**, *38*, 912.

23. Laughton, C. A.; Tanious, F.; Nunn, C. M.; Boykin, D. W.; Wilson, W. D.; Neidle, S. *Biochemistry* **1996**, *35*, 5655.

24. Ratmeyer, L.; Zapp, M.; Green, M.; Vinayak, R.; Kumar, A.; Boykin, D. W.; Wilson, W. D. *Biochemistry* **1996**, *35*, 13689.

25. Chandrasekaran, R.; Arnott, S. In *Landolt-Börnstein, New series, Group VII*; Saenger, W., Ed.; Springer-Verlag: Berlin, 1989; Vol. lb, p 68.

26. Veal, J. M.; Wilson, W. D. *J. Biomol. Struct. Dynam*. **1991**, *8*, 1119.

27. Sambrook, J.; Fritsch, E. F.; Maniatis, T. In *Molecular Cloning: A Laboratory Manual*; Nolan, C., Ed.; Cold Spring Harbor Laboratory: Plainview, 1988; p 6.36.

28. Ragunathan, K. G.; Schneider, H.-J. *Angew. Chem. Int. Ed. Engl.* **1996**, *35*, 1219 and references therein.